ISBN: 978-3-95450-231-8 ISSN: 2673-5490 doi: 10.18429/JACoW-IPAC2023-WEPA179

# MULTIPACTOR STUDIES FOR THE FCC–ee SUPERCONDUCTING SWELL CAVITIES

A. Plaçais*, F. Bouly, Y. Gómez Martínez, M. Meyer, CNRS-IN2P3, LPSC, Grenoble, France
A. Faus-Golfe, CNRS-IN2P3, IJCLab, Orsay, France
S. Gorgi Zadeh, F. Peauger, CERN, Geneva, Switzerland

*Abstract*

The Future Circular electron-positron Collider (FCC–ee) is a proposed new storage ring of 91 km circumference, which has been designed to carry out a precision study of Z, W, H, and ttbar with an extremely high-luminosity and unprecedented energy resolution. Given the high-energies, ranging from 45.6 to 183 GeV, the Synchrotron Radiation (SR) power is assumed to be limited to 50 MW per beam in all operation modes. A high-performance RF system based on Superconducting Cavities (SC) is supposed to compensate for SR losses. Different SC technologies are currently under study for such a system, the Slotted Waveguide ELLiptical (SWELL) being one of the possible solutions. In this paper, we numerically compute the position of the multipacting barriers of a SWELL cavity prototype, resonating at 1.3 GHz. We benchmark it against the TESLA cavity barriers, which are well documented. First results show that the SWELL cavity is less prone to multipacting in its operation range than the equivalent TESLA one.

## INTRODUCTION

The Slotted ELLiptical Waveguide (SWELL) is a promising superconducting radio-frequency (SRF) cavity design, based on the conceptual designs presented in [1, 2]. It operates in the $TM_{010}$ mode; it is composed of four open-structure quadrants, as shown in Fig. 1. It comprises four slots, which allow for an excellent Higher-Order Mode (HOM) transverse damping. It can operate both at high beam-current and at high accelerating gradient. Hence, it is a good candidate to have a single cavity type for the Z, W and H operating modes of FCC–ee; they are listed in Table 1 [3].

Table 1: RF voltage, beam current and accelerating field for the different operation modes of FCC–ee for a 600 MHz SWELL cavity [4].

| Mode | Z | W | H | ttbar |
|---|---|---|---|---|
| RF voltage [GV] | 0.120 | 1 | 2.08 | 11.3 |
| Beam current [mA] | 1280 | 135 | 26.7 | 5 |
| $E_{acc}$ [MV m$^{-1}$] | 2.67 | 10 | 12.5 | |

The SWELL cavity proposed for FCC–ee consists of two cells as shown in Fig. 1a, and works at 600 MHz [5, 6]. Under the framework of the FCC Feasibility Study, the CERN RF group designed a SWELL version of the middle-cell of the TESLA elliptical cavity [3, 7]. It resonates at 1.3 GHz, has a single cell and its slots are closed; it is represented in Fig. 1b. A Cu prototype of the 1.3 GHz cavity has been fabricated, assembled and tested with success at CERN [8]. The LPSC and the IJCLab laboratories are contributing to this effort by studying the multipacting in the SWELL cavity.

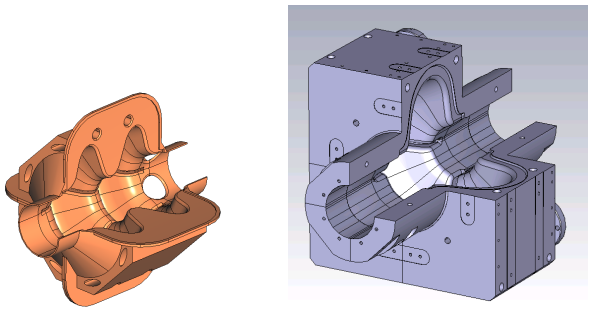

(a) SWELL 600 MHz two-cells.

(b) SWELL 1.3 GHz mono-cell prototype, that we study in this paper.

Figure 1: Representations of the SWELL cavities. Three quadrants over four are shown. Notice the different scales between the cartoons (a) and (b).

The multipacting is a parasitic resonant effect that can occur in RF systems under vacuum. It prevents the cavity from reaching its nominal field, creates a heat load on the walls of the cavity and degrades its quality factor. Even if multipacting was a significant issue in early cavities [9], it is generally considered that it can be mitigated in elliptical cavity shapes [10]. Nonetheless, it is important to quantify the apparition of this phenomenon in every new cavity design. Furthermore, the SWELL's HOM damping slots are a feature that could favor the multipacting apparition.

In this paper, we study the multipacting in the SWELL 1.3 GHz prototype. We use the TESLA elliptical cavity as a benchmark, where multipacting was experimentally observed for accelerating fields in the $17-22$ MV m$^{-1}$ range [10–13].

## NUMERICAL TOOLS SET UP AND INPUTS

We computed the field maps in the SWELL prototype and in the TESLA cavity with the eigenmode solver of CST Microwave Studio [14]; the geometry was imported in the form of a `STEP` file. Then, we used the Particle-in-Cell (PIC) solver of CST to compute the evolution of the electron population with time $n(t)$. For every simulation, we computed

* placais@lpsc.in2p3.fr

ISBN: 978-3-95450-231-8 ISSN: 2673-5490 doi: 10.18429/JACoW-IPAC2023-WEPA179



the exponential growth factor $\alpha$, defined as:

$$\bar{n}(t) = \bar{n}(t_0)\mathrm{e}^{\alpha t} \quad t \in [t_0, t_1] \tag{1}$$

where $\bar{n}(t)$ is the number of electrons averaged over an RF period. $t_0$ is the time at the beginning of the multipactor exponential growth. $t_1$ is the simulation end time. We studied accelerating fields ranging from 1 to 30 MV m$^{-1}$, which covers the SWELL operating range as well as the TESLA multipacting zone.

Electron emission is the phenomenon at the origin of the electron population growth. It takes place in the first nanometres of the material, and it is hereby extremely sensitive to the presence of contaminants [15]. Its main figure of merit is the Total Electron Emission Yield (TEEY, $\sigma$), which corresponds to the number of emitted electrons per incident electron. Emitted electrons can be secondary electrons, elastically backscattered electrons or inelastically backscattered electrons; they are not discriminated from each other in this study.

The SRF SWELL cavity is made of copper, with a very thin layer of pure niobium deposited on the inner wall by sputtering. Due to the thickness of the Nb layer, the Cu substrate does not influence the electron emission properties. Here, we take the TEEY of three different bulk Nb samples as input for the simulation. They went under different treatments and show different surface states. "Degreased" sample was simply degreased, and thus still holds its contamination layer [16]. "Baked out" sample was baked out at 300 °C, which removed most of its contaminants [17, 18]. "Sputtered" was electropolished and shows very little contamination [16]. We represented in Fig. 2 the TEEY as a function of the energy of incident electrons, at normal incidence, for this three materials. In our simulations, we modelled the TEEY with modified Vaughan model [19, 20]. We used a mean electron emission energy of 7.5 eV.

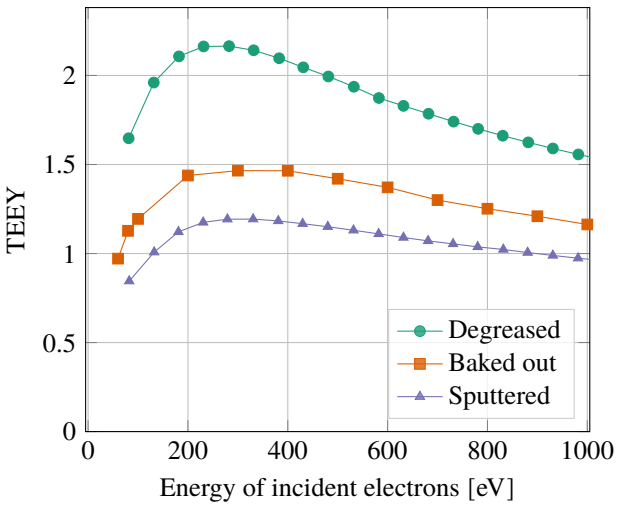


Figure 2: TEEY used for simulations. Degreased and sputtered data are taken from Ref. [16], and baked out from Ref. [17, 18].

## EXPONENTIAL GROWTH FACTORS

### *CST Microwave Studio Eigenmode Simulations*

We computed the electromagnetic field in the cavities under study with the CST eigenmode solver, after extensive convergence studies. We used a tetrahedral mesh; we observed that calculating the field map with a hexahedral mesh ultimately led to higher variations of $\alpha$ from one PIC simulation to another. We observed that the angle between two sectors was a critical parameter; we set it to 1°, which is the lowest possible. It reaches a conclusion from Ref. [21], where the electromagnetic fields were calculated with HFSS. We also observed that introducing symmetry planes was necessary. Omitting them led to important and unphysical electric field peaks and thus to unreasonable values of $E_{\mathrm{pk}}/E_{\mathrm{acc}}$ and $H_{\mathrm{pk}}/E_{\mathrm{acc}}$, which also favored the apparition of the multipacting. It is perhaps because the geometry files are created with another software and imported into CST.

### *CST Microwave Studio PIC Simulations*

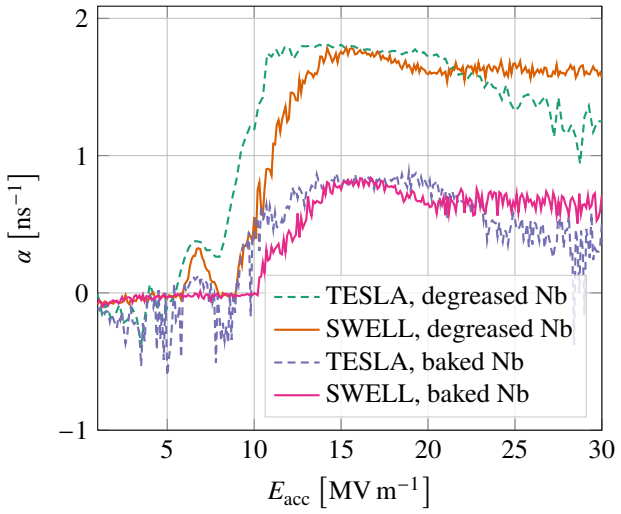


Figure 3: Exponential growth factor as a function of the accelerating field calculated with CST Microwave Studio. The cavities are the TESLA mono-cell 1.3 GHz and the SWELL mono-cell 1.3 GHz. Results for the sputtered Nb are not represented as no multipacting was detected.

We used a hexahedral mesh for the PIC simulations; tetrahedral meshes are not supported for this solver. We represented in Fig. 3 the exponential growth factors calculated with CST Microwave Studio data, as a function of the accelerating field. As expected, the multipacting is the most marked with the degreased Nb, which has the highest TEEY. For some simulations, all electrons were rapidly collected and values of $\alpha$ were not consistent. It is the case for all sputtered Nb simulations (not represented in Fig. 3) and for SWELL baked Nb at $E_{\mathrm{acc}} < 10$ MV m$^{-1}$. From a general point of view, the baked Nb $\alpha$ curves are more noisy. As a matter of a fact, with this material, the multipacting almost

ISBN: 978-3-95450-231-8 ISSN: 2673-5490 doi: 10.18429/JACoW-IPAC2023-WEPA179

does not exist and even a small decrease in TEEY led to the disappearance of the phenomenon.

For the TESLA cavity, we observe with baked and degreased Nb a first small multipactor barrier around 6 MV m$^{-1}$, and a second one at 8 MV m$^{-1}$ and onwards. As multipacting is expected to appear around 17 – 22 MV m$^{-1}$ [10–13], either our simulations overestimate the multipacting, or none of the TEEY that we used is representative of the cavities properties. It is also possible that both explanations are correct. The $\alpha$ curves for the SWELL follow the same tendency than the TESLA. Under 22 MV m$^{-1}$, multipacting is less marked in the SWELL than in the TESLA. In the contrary, it is more pronounced in the SWELL prototype for $E_{acc} > 22$ MV m$^{-1}$.

## DISCUSSION

Preliminary results would show that although the TEEY influences the amplitude of the multipacting, it does not seem to modify the shape of the $\alpha(E_{acc})$ curves. Firstly, the electron emission data available from literature is not valid in the very low impact energy range. We represented in Fig. 4 a histogram of the electrons impact energies during a CST PIC simulation, in the SWELL cavity and for $E_{acc} = 20$ MV m$^{-1}$. Material is baked Nb; we also represented the range of energies for which the electron emission data of this material is valid. There is a significant proportion of low-energy electrons, which fall out of this range. For degreased Nb, the first cross-over energy is even lower than the first measure point. Secondly, we did not use experimental data for the electron emission energy, nor for the TEEY at non-normal incidence. Both have a significant influence on the multipactor apparition [10, 22]. Thirdly, we did not discriminate backscattered electrons from secondaries which may influence the multipacting apparition dynamics [23, 24].

The material of the SWELL cavity is not bulk niobium, but Cu with sputtered Nb. They are not created through the same processes, and their surface state as well as their contaminations may be very different, and so will be their emission properties. Electron emission measurements on Nb/Cu samples will take place at ONERA Toulouse, France and IJCLab at Orsay, France by the end of the year. They will include measurements of TEEY at low energy, at different impact angles and of emission energy distribution.

We observed that the TESLA and SWELL prototype had similar $\alpha(E_{acc})$ curve shapes. For $E_{acc} < 22$ MV m$^{-1}$, the electron avalanche occurs on the whole equatorial plane, as represented in Fig. 5a. It is a two-point multipactor and is well documented in elliptical cavities. For a given value of accelerating field, the electric field is lower on the SWELL equator than on the TESLA equator; hence multipacting is more pronounced in the latter cavity. After 22 MV m$^{-1}$, the multipactor in the SWELL cavity appears around its slots; it is represented in Fig. 5b, and is a two-point multipactor as well. In contrary to what we first thought, multipacting does not appear inside the slots. Instead, all electrons that enter it go out of resonance and do not participate to the multipactor anymore. This type of multipacting does not concern the TESLA cavity and explain why SWELL is the most prone to multipactor at the highest values of $E_{acc}$.

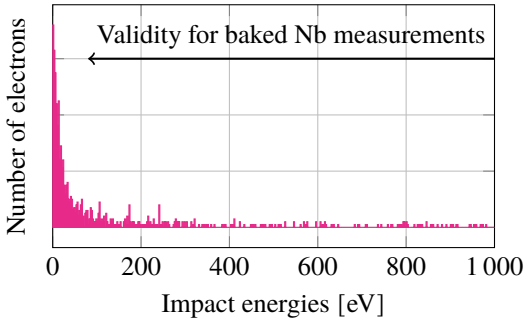


Figure 4: Histogram of the impact energies of electrons in the SWELL prototype, according to CST. Simulation realized at $E_{acc} = 20$ MV m$^{-1}$ with baked Nb.

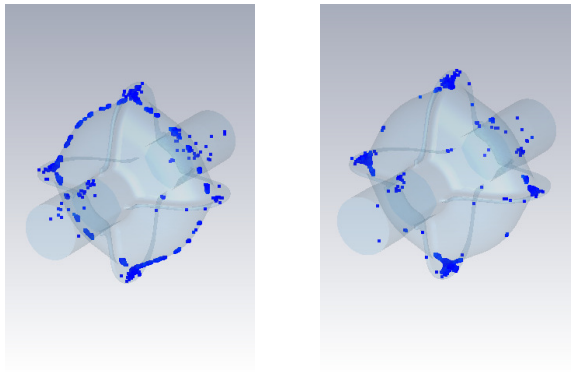

(a) $E_{acc} = 17$ MV m$^{-1}$: multipactor on the equatorial plane.

(b) $E_{acc} = 22$ MV m$^{-1}$: multipactor at the slots entrance.

Figure 5: Position of the electrons at the end of the CST simulations, for the SWELL cavity and degreased Nb.

## CONCLUSION

In this paper, we studied the multipacting in the SWELL 1.3 GHz prototype and in the benchmark TESLA cavity. We used the numerical simulation tool CST Microwave Studio. We observed that multipacting was less marked in the SWELL prototype than in the TESLA at accelerating fields lower than 22 MV m$^{-1}$, where SWELL will be exploited.

In order to consolidate this study, a similar set of simulations with SPARK3D is ongoing. Electron emission measurements on Nb/Cu samples will be led at the ONERA Toulouse and at IJCLab; it will allow us to realize a new set of simulations, with a more realistic electron emission model. We will also perform multipacting measurements on the SWELL prototype at the CERN by the end of the year – fabrication of the Cu prototype is finished, and deposition of the Nb film is about to start [8]. Finally, we plan to realize multipacting studies for the two-cell 600 MHz SWELL cavity as well.

ISBN: 978-3-95450-231-8 ISSN: 2673-5490 doi: 10.18429/JACoW-IPAC2023-WEPA179



# REFERENCES


[1] "High RF Power Production for CLIC," in *Proc. PAC'07*, Albuquerque, NM, USA, Jun. 2007, pp. 2194–2196. https://jacow.org/p07/papers/WEPMN071.pdf

[2] Z. Liu and A. Nassiri, "Novel superconducting rf structure for ampere-class beam current for multi-GeV energy recovery linacs," *Physical Review Special Topics - Accelerators and Beams*, vol. 13, no. 1, p. 012 001, 2010. doi:10.1103/PhysRevSTAB.13.012001

[3] F. Peauger, S. Gorgi Zadeh, G. Campbell Burt, M. Timmins, and M. Therasse, "The SWELL cavities program: The SWELL cavity development plan," in *FCC Week 2022*, 2022.

[4] F. Peauger *et al.*, "SWELL and Other SRF Split Cavity Development," in *Proc. LINAC'22*, Liverpool, UK, 2022, pp. 300–304. doi:10.18429/JACoW-LINAC2022-TU1AA04

[5] I. Syratchev, F. Peauger, I. Karpov, and O. Brunner, "A Superconducting Slotted Waveguide Elliptical Cavity for FCC-ee," Tech. Rep., 2021. doi:10.5281/ZENODO.5031953

[6] S. G. Zadeh, O. Brunner, F. Peauger, and I. Syratchev, "Optimization of a 600 MHz Two-Cell Slotted Waveguide Elliptical Cavity for FCC-ee," in *Proc. IPAC'22*, Bangkok, Thailand, 2022, pp. 1323–1326. doi:10.18429/JACoW-IPAC2022-TUPOTK048

[7] S. Gorgi Zadeh, F. Peauger, G. Campbell Burt, M. Timmins, M. Therasse, and T. Koettig, "The SWELL cavities program: The SWELL cavity RF design," in *FCC Week 2022*, 2022.

[8] K. Scibor *et al.*, "SWELL 1.3 GHz Cavity fabrication approach and machining," presented at IPAC'23, Venice, Italy, May 2023, paper THPM016, this conference.

[9] H. S. Padamsee, *RF superconductivity*. Wiley-VCH, 2009.

[10] V. D. Shemelin and S. A. Belomestnykh, *Multipactor in Accelerating Cavities*. Springer International Publishing, 2020. doi:10.1007/978-3-030-48198-8

[11] P. Ylä-Oijala, "Electron Multipacting in TESLA Cavities and Input Couplers," *Patricle Accelerators*, vol. 63, pp. 105–137, 1999. http://cds.cern.ch/record/1120324/files/p105.pdf

[12] K. Saito, "Experimental Formula of the on-set Level of Two-point Multipacting Over the RF Frequency Range 500 MHz to 1300 MHz," in *Proc. SRF'01*, Tsukuba, Japan, Sep. 2001, pp. 419–422. https://jacow.org/srf01/papers/PR019.pdf

[13] K. Twarowski, L. Lilje, and D. Reschke, "Multipacting in 9-cell Tesla Cavities," in *Proc. SRF'03*, Lübeck, Germany, Sep. 2003, pp. 733–735. https://jacow.org/SRF2003/papers/THP41.pdf

[14] Dassault Systèmes, *CST Microwave Studio*, 2023.

[15] T. Gineste, M. Belhaj, G. Teyssedre, and J. Puech, "Investigation of the electron emission properties of silver: From exposed to ambient atmosphere Ag surface to ion-cleaned Ag surface," *Applied Surface Science*, vol. 359, pp. 398–404, 2015. doi:10.1016/j.apsusc.2015.10.121

[16] S. Aull, T. Junginger, H. Neupert, and J. Knobloch, "Secondary Electron Yield of SRF Materials," in *Proc. SRF'15*, Whistler, Canada, Sep. 2015, pp. 686–690. https://jacow.org/SRF2015/papers/TUPB050.pdf

[17] R. Calder, G. Dominichini, and N. Hilleret, "Influence of various vacuum surface treatments on the secondary electron yield of niobium," *Nuclear Instruments and Methods in Physics Research Section B: Beam Interactions with Materials and Atoms*, vol. 13, no. 1-3, pp. 631–636, 1986. doi:10.1016/0168-583X(86)90581-1

[18] H. Piel, "Superconducting cavities," CERN, Tech. Rep., 1988, pp. 149–196. doi:10.5170/CERN-1989-004

[19] J. Vaughan, "A new formula for secondary emission yield," *IEEE Transactions on Electron Devices*, vol. 36, no. 9, pp. 1963–1967, 1989. doi:10.1109/16.34278

[20] C. P. Vicente *et al.*, "Multipactor breakdown prediction in rectangular waveguide based components," in *IEEE MTT-S International Microwave Symposium Digest, 2005.*, vol. 2005, 2005, pp. 1055–1058. doi:10.1109/MWSYM.2005.1516852

[21] S. Kazakov, I. V. Gonin, and V. P. Yakovlev, "Multipactor Simulation in SC Elliptical Shape Cavities," in *Proc. IPAC'12*, New Orleans, LA, USA, May 2012, pp. 2327–2329. https://jacow.org/IPAC2012/papers/WEPPC051.pdf

[22] W. Weingarten, "Electron Loading," in *Proc. SRF'84*, Geneva, Switzerland, Jul. 1984, pp. 551–582. https://jacow.org/srf84/papers/SRF84-30.pdf

[23] R. Seviour, "The role of elastic and inelastic electron reflection in multipactor discharges," *IEEE Transactions on Electron Devices*, vol. 52, no. 8, pp. 1927–1930, 2005. doi:10.1109/TED.2005.851854

[24] A. Plaçais, M. Belhaj, J. Hillairet, and J. Puech, "A three-dimensional Dionne model for multipactor simulations," *Physics of Plasmas*, vol. 27, no. 5, p. 053 512, 2020. doi:10.1063/5.0004076